1521-0111/88/3/488–501$25.00
MOLECULAR PHARMACOLOGY

http://dx.doi.org/10.1124/mol.115.099176
Mol Pharmacol 88:488–501, September 2015

Structure-Function Basis of Attenuated Inverse Agonism of Angiotensin II Type 1 Receptor Blockers for Active-State Angiotensin II Type 1 Receptor[S]

Takanobu Takezako, Hamiyet Unal, Sadashiva S. Karnik, and Koichi Node

Department of Advanced Heart Research, Saga University, Saga, Japan (T.T.); Department of Cardiovascular Medicine, Saga University, Saga, Japan (K.N.); Department of Molecular Cardiology, Lerner Research Institute, Cleveland Clinic Foundation, Cleveland, Ohio (H.U., S.S.K.); Department of Biosignal Pathophysiology, Kobe University Graduate School of Medicine, Kobe, Japan (T.T.); and Department of Basic Sciences, Faculty of Pharmacy and Betul Ziya Eren Genome and Stem Cell Center, Erciyes University, Kayseri, Turkey (H.U.)

Received April 1, 2015; accepted June 29, 2015

ABSTRACT

Ligand-independent signaling by the angiotensin II type 1 receptor (AT1R) can be activated in clinical settings by mechanical stretch and autoantibodies as well as receptor mutations. Transition of the AT1R to the activated state is known to lower inverse agonistic efficacy of clinically used AT1R blockers (ARBs). The structure-function basis for reduced efficacy of inverse agonists is a fundamental aspect that has been understudied not only in relation to the AT1R but also regarding other homologous receptors. Here, we demonstrate that the active-state transition in the AT1R indeed attenuates an inverse agonistic effect of four biphenyl-tetrazole ARBs through changes in specific ligand-receptor interactions. In the ground state, tight interactions of four ARBs with a set of residues ($Ser109^{TM3}$, $Phe182^{ECL2}$, $Gln257^{TM6}$, $Tyr292^{TM7}$, and $Asn295^{TM7}$) results in potent inverse agonism. In the activated state, the ARB-AT1R interactions shift to a different set of residues ($Val108^{TM3}$, $Ser109^{TM3}$, $Ala163^{TM4}$, $Phe182^{ECL2}$, $Lys199^{TM5}$, $Tyr292^{TM7}$, and $Asn295^{TM7}$), resulting in attenuated inverse agonism. Interestingly, V108I, A163T, N295A, and F182A mutations in the activated state of the AT1R shift the functional response to the ARB binding toward agonism, but in the ground state the same mutations cause inverse agonism. Our data show that the second extracellular loop is an important regulator of the functional states of the AT1R. Our findings suggest that the quest for discovering novel ARBs, and improving current ARBs, fundamentally depends on the knowledge of the unique sets of residues that mediate inverse agonistic potency in the two states of the AT1R.

Introduction

G Protein–coupled receptors (GPCRs) constitute one of the largest gene superfamilies in the human genome (Fredriksson et al., 2003). GPCRs are activated by ligands such as ions, neurotransmitters, peptides, and proteins as well as by sensory agents such as photons, touch, taste, and smell. Activation of GPCRs is a fundamental mechanism that promotes intracellular signaling in numerous physiologic and pathologic processes. Therefore, drugs that interfere with mechanisms of the GPCR activation are important tools in combating disease. Indeed, approximately 26% of clinically available drugs are known to target GPCRs (Garland, 2013).

The angiotensin II (Ang II) type 1 receptor (AT1R) is an extensively studied GPCR in the context of ligand-mediated and ligand-independent mechanisms of receptor activation (Unal et al., 2012; Unal and Karnik, 2014). It is the primary receptor for Ang II, a peptide hormone produced by the renin-angiotensin system and the antihypertension drugs known as AT1R blockers (ARBs). The AT1R is the principal regulator of blood pressure and body-fluid homeostasis, and it plays vital roles in cardiovascular and renal pathophysiology. Overstimulation of AT1R is implicated in hypertension, coronary artery disease, cardiac hypertrophy, heart failure, arrhythmia, stroke, diabetic nephropathy, and ischemic heart and renal disease states, which can be greatly reduced by treatment with ARBs (Khan, 2011; Vijayaraghavan and Deedwania, 2011; Lee et al., 2012; Vejakama et al., 2012). The ARBs are nonpeptide receptor inhibitors with a common biphenyl-tetrazole scaffold, including the well known clinically used antihypertension drugs Losartan, Candesartan,

This work was supported by a Grant-in-Aid for Research Activity Start-up [Grant 18890141] to T.T. from the Ministry of Education, Culture, Sports, Science and Technology in Japan. This work was supported in part by a National Institutes of Health R01 Grant [Grant R01-HL57470] to S.S.K. and a National Research Service Award [HL007914] to H.U. K.N. was financially supported by contributions from Merck & Co., Inc., Shionogi & Co., Ltd., and Novartis Pharma K.K.

T.T., H.U., and S.S.K. contributed equally to this work.

dx.doi.org/10.1124/mol.115.099176.

[S] This article has supplemental material available at molpharm.aspetjournals.org.

ABBREVIATIONS: Ang II, angiotensin II; ARB, angiotensin II type 1 receptor blocker; AT1R, angiotensin II type 1 receptor; DMEM, Dulbecco's modified Eagle's medium; ECL2, second extracellular loop; EXP3174, 2-butyl-5-chloro-3-[[4-[2-(2*H*-tetrazol-5-yl)phenyl]phenyl]methyl]imidazole-4-carboxylic acid; GPCR, G protein–coupled receptor; H-bond, hydrogen bond; IP, inositol phosphate; TM, transmembrane; WT, wild-type; ZD7155, 5,7-diethyl-3,4-dihydro-1-[[2′-(1*H*-tetrazol-5-yl)[1,1′-biphenyl]-4-yl]methyl]-1,6-naphthyridin-2(1*H*)-one hydrochloride.

Valsartan, Irbesartan, Telmisartan, Eprosartan, Olmesartan, and Azilsartan.

The AT1R activates the heterotrimeric G protein $G_{q/11}$, leading to inositol phosphate (IP) signaling. Typically, Ang II binding induces the active conformation of the AT1R; however, recent studies have demonstrated that both mechanical stress and AT1R-directed autoantibodies can activate the AT1R, independent of agonist binding (Mederos y Schnitzler et al., 2011; Storch et al., 2012; Unal et al., 2012; Wallukat and Schimke, 2014). Both modes of ligand-independent activation of AT1R may occur clinically as in hypertension, preecclampsia, or cardiac overload conditions, which can be attenuated by actions of inverse agonists such as Candesartan (Zou et al., 2004; Wei et al., 2011). Mutations produce ligand-independent activation in the AT1R by inducing conformational changes in the receptor, and in this state the binding affinity of the AT1R for ARBs is known to reduce significantly (Noda et al., 1996; Le et al., 2003). However, the molecular basis for a decrease in the affinity of activated GPCRs toward inverse agonists has not been studied in the AT1R, and in general this aspect is understudied in the entire GPCR superfamily. We hypothesize that interactions that determine the inverse agonism of an ARB differ in the active state compared with the ground state of a GPCR owing to the conformational change associated with the active state transition. To test this hypothesis in the present study, we combine mutagenesis (Fig. 1A), ligand-binding and IP production assays, and molecular modeling to understand the structural basis of inverse agonism for four biphenyl-tetrazol ARBs (Fig. 1B) evaluated in wild-type (WT) and constitutively activated mutant N111G-AT1R. Our findings indicate that different sets of residues mediate inverse agonism of ARBs in the two states of the AT1R.

Materials and Methods

Ang II and [Sar^1, Ile^8]Ang II were purchased from Bachem (Bubendorf, Switzerland). ^{125}I-[Sar^1, Ile^8]Ang II (specific activity, 2,200 Ci/mmol) was purchased from Dr. Robert Speth (Peptide Radioiodination Service Center, University of Mississippi, University, MS). Losartan and EXP3174 [2-butyl-5-chloro-3-[[4-[2-(2*H*-tetrazol-5-yl)phenyl]phenyl]methyl]imidazole-4-carboxylic acid] were gifted from Merck & Co. (Kenilworth, NJ). Valsartan and Irbesartan were gifted from Novartis Pharmaceuticals (Cambridge, MA) and Sanofi Aventis (Paris, France), respectively. Myo-[2-^{3}H(N)]Inositol was purchased from GE Healthcare Life Science (Little Chalfont, UK). COS-1 cells were purchased from the European Collection of Cell Culture (Salisbury, UK). The FuGENE 6 transfection reagent was purchased from Roche Diagnostics (Indianapolis, IN).

Mutagenesis, Expression, and Membrane Preparation. The synthetic rat AT1R gene, cloned in the shuttle expression vector pMT-3, was used for the expression and mutagenesis as previously described (Noda et al., 1996). We mutated the residues that are shown as the binding site residues for ARBs by previous experimental and modeling studies. For each residue, we substituted a side chain with nearly the same size and/or chemical characteristics. For instance, Asn is replaced with Ala, which has a similar size but cannot form a hydrogen bond (H-bond). The Lys side chain is replaced with Gln, which has a similar size but cannot form a salt bridge, as described in previous mutagenesis studies (Yamano et al., 1992; Ji et al., 1994, 1995; Schambye et al., 1994; Noda et al., 1995; Gosselin et al., 2000; Takezako et al., 2004; Baleanu-Gogonea and Karnik, 2006; Tuccinardi et al., 2006). To express the AT1R protein, 10 μg of purified plasmid DNA per 10^7 cells was used in the transfection. COS1 cells cultured in Dulbecco's modified Eagle's medium (DMEM) supplemented with 10% fetal bovine serum were transfected using the FuGENE6 transfection reagent for membrane preparation. The transfected cells were cultured for 48 hours and then harvested, and the nitrogen Parr bomb disruption method was used in the presence of protease inhibitors to prepare the cell membranes. The receptor expression was assessed in each case according to immunoblot analysis and ^{125}I-[Sar^1, Ile^8]Ang II saturation binding analysis.

Competition Binding Assay. The ^{125}I labeled [Sar^1, Ile^8]Ang II binding experiments were carried out under equilibrium conditions as previously described (Takezako et al., 2004).

Inositol Phosphate Production Assay. Semiconfluent AT1R-transfected COS1 cells seeded in 6-well plates were labeled for 24 hours with myo-[2-^{3}H(N)]-Inositol (1.5 μCi/ml; specific activity, 22 μCi/mol) at 37°C in DMEM supplemented with 10% fetal bovine serum. The labeled cells were washed two times with DMEM and incubated with DMEM containing 10 mM LiCl and vehicle or 1 μM of Ang II for various time intervals between 5 and 120 minutes at 37°C. To examine the inverse agonist activity, the cells were preincubated with DMEM containing vehicle or various concentrations of each ligand for 30 minutes at 37°C. A total of 10 mM LiCl was subsequently added, and the incubation was continued for a further 120 minutes at 37°C. At the end of the incubation, the medium was removed, and the total soluble IP was extracted from the cells using perchloric acid extraction, as previously described (Noda et al., 1996). The EC_{50} and IC_{50} values were calculated according to a nonlinear regression analysis using the GraphPad Prism software program (GraphPad, La Jolla, Ca). The inverse agonist activity of the ARBs for each mutant was calculated as a percent of receptor activity of vehicle-treated cell expressing each mutant (constitutive activity of each mutant). We defined vehicle-treated 0% constitutive activity for each mutant receptor. Therefore, −10% inverse agonist activity means 90% of constitutive activity and −100% of inverse agonist activity means 0% of constitutive activity. In other words, −100% inverse agonist activity means complete suppression of the constitutive activity for the WT or mutant examined.

Models of the AT1R Ligand-Binding Pocket with ARBs. Models of the binding pocket for Losartan, EXP3174, Valsartan, and Irbesartan were constructed as described in Zhang et al. (2015). The AT1R crystal structure was used to dock these four ARBs through an energy-based docking protocol in the ICM molecular modeling software suite provided by Molsoft (San Diego, CA). The initial model for each ARB was optimized by adding side chain hydrogen atoms, followed by optimization of the conformations generated and by generation of soft potential maps in a $30 \times 30 \times 30$ Å^3 box that covered the extracellular half of the receptor. Molecular models of compounds were generated from two-dimensional representations and their three-dimensional geometry was optimized using the Merck molecular force field 94 force field (Halgren, 1995). Molecular docking employed biased probability Monte Carlo optimization of the ligand internal coordinates in the grid potentials of the receptor (Abagyan and Totrov, 1997). Five independent docking runs were performed for each ligand starting from a random conformation; Monte Carlo sampling and optimization was performed at high thoroughness set to 30. We treated the Lys199$^{5.42}$ side chain as a flexible group in the receptor, allowing these side chain rotamers to freely sample the space. Up to 30 alternative complex conformations of the ligand-receptor complex were generated and rescored using the ICM binding score function, which accounts for Van der Waals, electrostatic, H-bonding, nonpolar and polar atom solvation energy differences between bound and unbound states, the ligand internal strain, conformational entropy, and ligand- and receptor-independent constants. The results of individual docking runs for each ligand were considered consistent if at least three of the five docking runs produced similar ligand conformations (root mean square deviation $<$ 2.0 Å) and binding score <-20.0 kJ/mol in three out of five trials. The unbiased docking procedure did not use distance restraints or any other a priori derived information for the ligand-receptor interactions.

Statistical Analysis. All data are presented as the mean ± S.E.M. of at least three independent experiments performed in duplicate. Multiple comparisons were made using a one-way analysis of variance

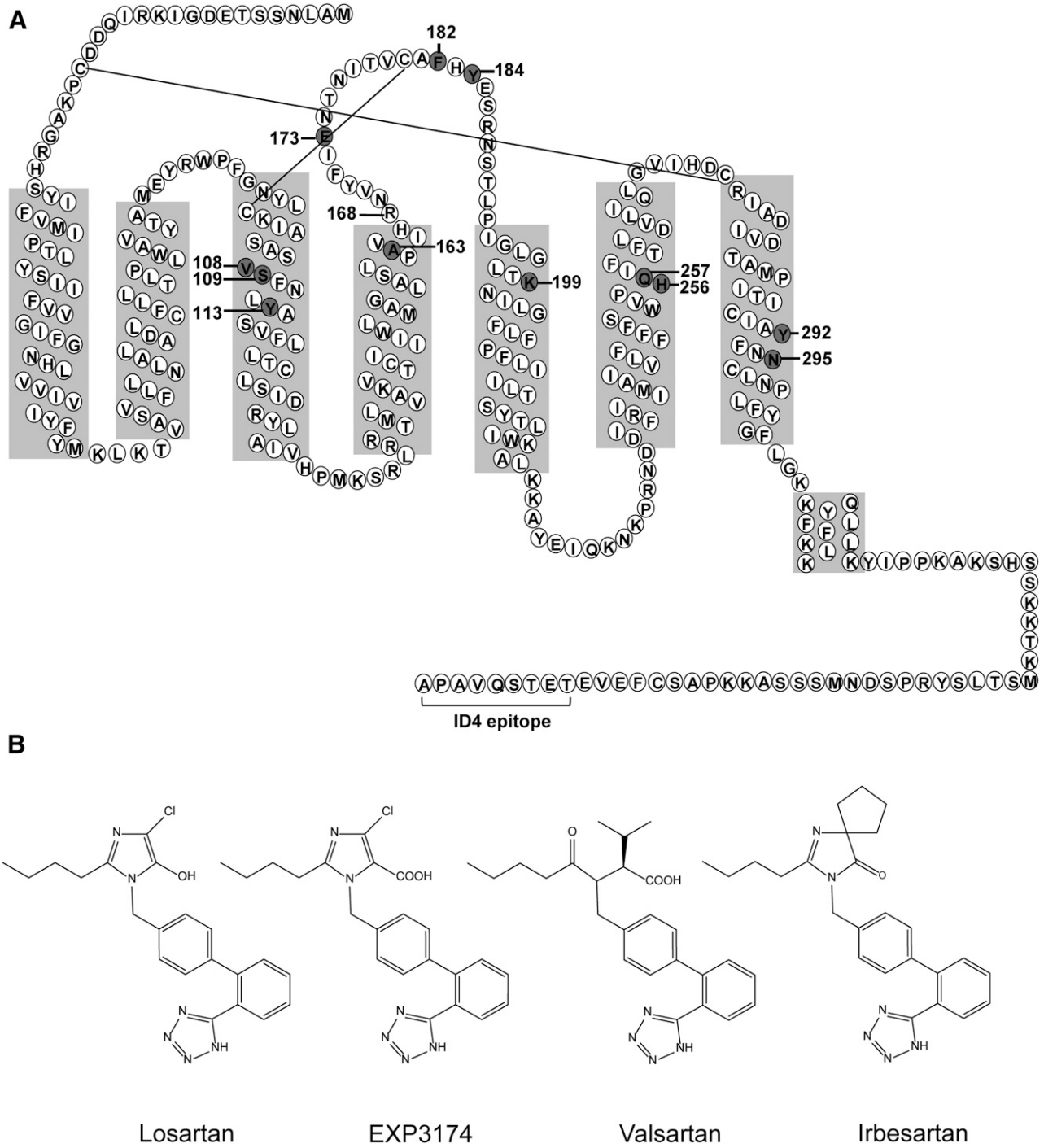

Fig. 1. Structures of the AT1R and four biphenyl-tetrazole group ARBs. (A) Secondary structure model of rat AT1R revised based on the crystal structure of human AT1R. Residues that were mutated in this study are numbered and highlighted. The epitope tag attached at the C-terminal end for detection by the ID4 monoclonal antibody is underlined. The attachment of this sequence does not alter the properties of the AT1R (Takezako et al., 2004). (B) Chemical structures of Losartan, EXP3174, Valsartan, and Irbesartan. All four ARBs share a structure with the biphenyl-tetrazole group.

followed by the Bonferroni post hoc test or Dunnett's post hoc test. P values of <0.05 were considered to be statistically significant.

Results

Prolonging Incubation Increases the Constitutive Activity of WT AT1R. We used the WT AT1R (WT-AT1) as a ground state receptor and constitutively active N111G mutant AT1R (N111G-AT1), which mimics activated AT1R conformation (Boucard et al., 2003; Martin et al., 2004, 2007; Unal et al., 2013), as an activated state receptor. Previous studies have reported that WT-AT1 displays only a modest constitutive activity (Miura et al., 2006, 2008). To examine the inverse agonist activity for the ground state AT1R with adequate sensitivity, we prolonged the incubation period during IP measurement to take advantage of the cumulative constitutive activity optimized to an adequate level. The constitutive IP production was increased in a linear fashion as

the incubation period increased in the WT-AT1, reaching the highest total IP level following a 120-minute incubation period (Supplemental Fig. 1). Hence, the following experiments were performed using the 120-minute incubation time.

Differences in the Pharmacological Properties of the ARBs between WT-AT1 and N111G-AT1. The pharmacological properties of the ARBs Losartan, EXP3174, Valsartan, and Irbesartan (Fig. 2A) were compared between WT-AT1 and N111G-AT1. The binding affinity of all four ARBs was higher for WT-AT1 than for N111G-AT1. The order of the binding affinity of the four ARBs for WT-AT1 was the same as that for N111G-AT1. The order of the binding affinity was Irbesartan > EXP3174 > Valsartan > Losartan for both WT-AT1 and N111G-AT1 (Tables 1 and 2). All four ARBs showed inverse agonist activity in a concentration-dependent manner for both WT-AT1 and N111G-AT1. The order of potency observed from EC_{50} toward WT-AT1 and N111G-AT1 is different for the four ARBs. The order of potency observed toward WT-AT1 for the four ARBs is EXP3174 = Valsartan = Irbesartan > Losartan (Fig. 2A). On the other hand, the order of potency toward N111G-AT1 for the four ARBs is EXP3174 = Irbesartan > Valsartan > Losartan (Fig. 2A). As anticipated, the inverse agonist efficacy (i.e., maximal inhibition) of all four ARBs was stronger for WT-AT1 than for N111G-AT1 and the efficacy of the four ARBs for N111G-AT1 differed from WT-AT1. The efficacy of EXP3174 > Valsartan = Losartan = Irbesartan for WT-AT1 and EXP3174 = Valsartan > Losartan = Irbesartan for N111G-AT1 (Fig. 2B). These pharmacological differences suggest that the degree of transition of the AT1R toward an activated state may alter the binding mode of the four ARBs.

Residues Specific for Binding of Ligands in WT-AT1. To identify the residues specific for the binding of ligands in WT-AT1, the effects of various mutants introduced in the WT-AT1 background (WT-BG) on the binding affinity of the ligands were examined (Table 1). Since ARBs make contact with several residues in the AT1R and the change of some contact residues shows a small reduction of ligand-binding affinity, we used the effect of a known change to set the 3-fold change as the cutoff. For example, substitution of Lys199 for an Ala reduced the binding affinity of Losartan by about 3-fold compared with WT-AT1R (Table 1). Therefore, we consider the 3-fold change in binding as a functionally important change because close, small structural differences

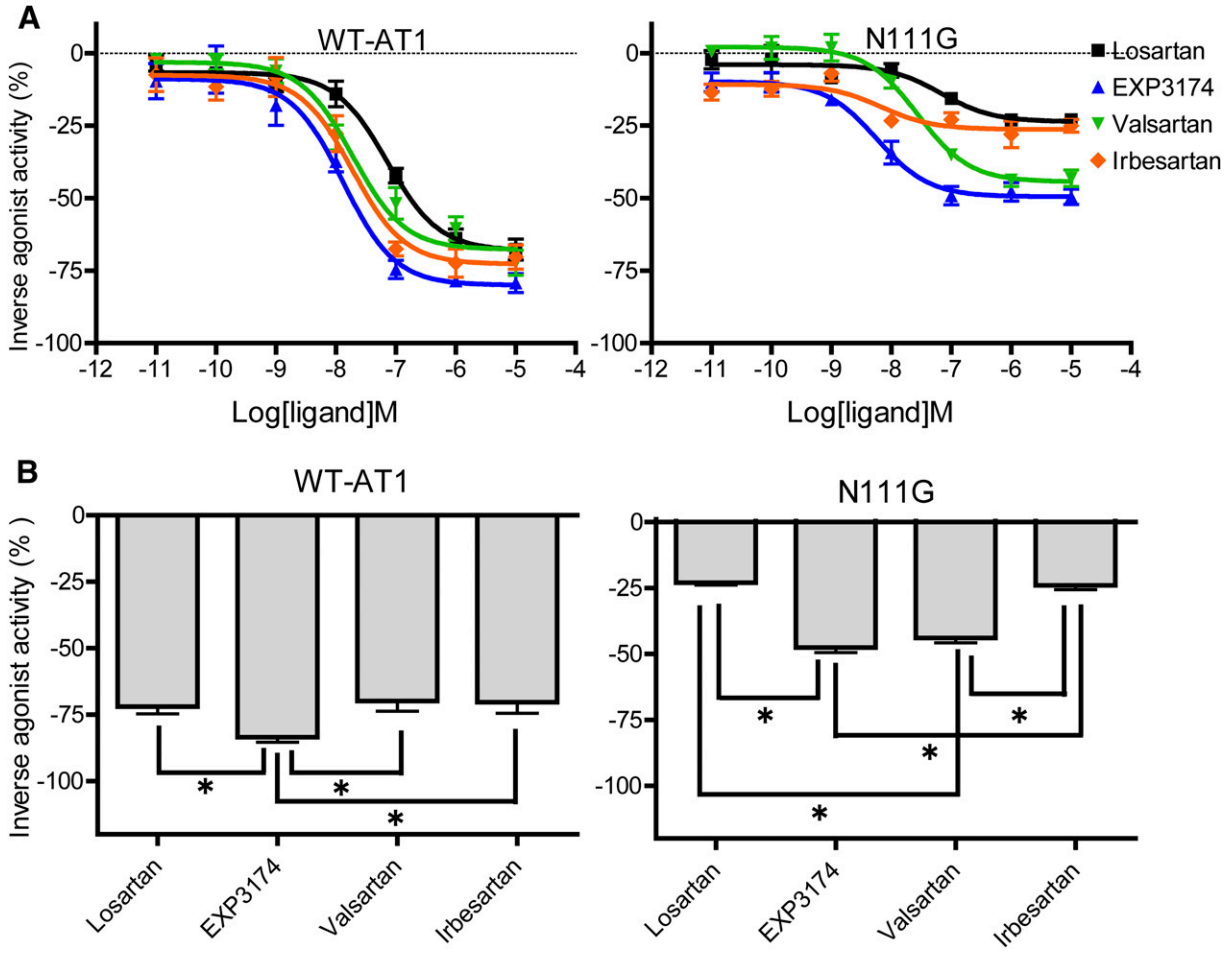

Fig. 2. Differences in the inverse agonist properties of the four ARBs for WT-AT1 and mutant N111G as measured by IP assay. (A) Concentration-dependent inverse agonist activity of Losartan, EXP3174, Valsartan, and Irbesartan for WT-AT1 (left panel) and mutant N111G-transfected (right panel) COS1 cells. (B) Maximal inverse agonist activity of Losartan, EXP3174, Irbesartan, and Valsartan for WT-AT1 (left panel) and mutant N111G (right panel) was measured at a concentration of 10 μM of each ARB. The inverse agonist activity of four ARBs is expressed as the percent of the constitutive activity of the vehicle-treated WT-AT1 and N111G-AT1–transfected COS1 cells, respectively. The constitutive activity of the vehicle-treated WT-AT1 and N111G-AT1 cells is defined as 0%. *$P < 0.05$.

TABLE 1

Ligand-binding properties of the WT and mutants in the WT background AT1R

The values are presented as the mean ± S.E.M. of at least three independent experiments performed in duplicate. The effect of the mutations on the binding affinity is expressed as $\Delta K_i = K_i(\text{mutant})/K_i(\text{WT-AT1})$.

Mutation	Location	B_{max}	Angiotensin II		Losartan		EXP3174		Valsartan		Irbesartan	
			K_i	ΔK_i	K_i	ΔK_i	K_i	ΔK_i	K_i	ΔK_i	K_i	ΔK_i
		pmol/mg	*nM*		*nM*		*nM*		*nM*		*nM*	
WT-AT1		2.62 ± 0.16	0.9 ± 0.2	1	10.7 ± 1.3	1	1.0 ± 0.1	1	2.9 ± 0.3	1	0.25 ± 0.01	1
V108I	TM3	2.68 ± 0.49	1.6 ± 0.4	1.8	1087 ± 165	101	47.7 ± 5.1	47.7	316 ± 24.4	109	23.2 ± 0.8	77.3
S109T	TM3	1.21 ± 0.49	1.9 ± 1.0	2.1	8649 ± 1654	808	803 ± 220	803	5707 ± 1538	1968	328 ± 52.4	1093
Y113A	TM3	1.49 ± 0.06	12.0 ± 5.2	13.6	2068 ± 331	193	384 ± 165	384	2190 ± 101	755	62.6 ± 16.9	209
A163T	TM4	1.04 ± 0.12	1.6 ± 0.5	1.8	120 ± 5.5	11.2	9.6 ± 1.9	9.6	20.8 ± 2.6	7.2	3.1 ± 1.3	10.3
E173A	ECL2	4.34 ± 0.29	2.1 ± 1.0	2.3	11.6 ± 2.6	1.1	0.7 ± 0.2	0.7	2.3 ± 1.0	0.8	0.18 ± 0.02	0.7
F182A	ECL2	4.45 ± 0.95	17.0 ± 1.3	18.3	25.1 ± 3.7	2.3	1.1 ± 0.2	1.1	6.1 ± 1.2	2.1	0.30 ± 0.05	1
Y184A	ECL2	1.53 ± 0.13	12.6 ± 0.3	14	8.8 ± 1.9	0.8	0.6 ± 0.1	0.6	2.9 ± 0.03	1	0.044 ± 0.007	0.1
K199A	TM5	0.08 ± 0.01	19.9 ± 5.8	22.1	35.4 ± 11.4	3.3	17.1 ± 2.0	17.1	214 ± 102	73.8	0.31 ± 0.06	1
K199Q	TM5	0.28 ± 0.14	16.3 ± 2.8	18.1	16.8 ± 3.7	1.6	1.2 ± 0.5	1.2	10.4 ± 0.1	3.6	0.24 ± 0.08	0.7
H256A	TM6	1.63 ± 0.91	0.5 ± 0.0	0.6	11.0 ± 1.8	1	0.9 ± 0.1	0.9	3.8 ± 0.1	1.3	0.24 ± 0.02	0.7
Q257A	TM6	3.37 ± 0.18	1.1 ± 0.4	1.2	66.9 ± 4.7	6.3	14.5 ± 2.2	14.5	69.5 ± 6.4	24	0.46 ± 0.14	1.7
Q257E	TM6	2.23 ± 0.36	0.38 ± 0.004	0.4	131 ± 22.4	12.2	10.5 ± 2.7	10.5	39.5 ± 3.2	13.6	2.1 ± 0.9	7
Y292A	TM7	5.03 ± 0.62	1.2 ± 0.1	1.3	102 ± 18.5	9.5	3.0 ± 1.9	3	52.3 ± 6.6	18	4.3 ± 0.3	14.3
N295A	TM7	6.04 ± 1.83	8.7 ± 0.9	9.7	1461 ± 143	137	56.9 ± 12.3	56.9	227 ± 7.8	78.3	25.8 ± 4.4	86
S109T/A163T	TM3/TM4	3.54 ± 0.86	1.6 ± 0.1	1.8	4007 ± 597	375	290 ± 48.4	290	2602 ± 89.8	897	47.4 ± 2.7	158
S109T/H256A	TM3/TM6	0.41 ± 0.06	2.1 ± 0.8	2.3	11,664 ± 1400	1090	522 ± 95.0	522	6651 ± 762	2293	333 ± 124	1110
S109T/N295A	TM3/TM7	1.74 ± 0.31	2.0 ± 0.6	2.2	576,050 ± 26,509	53,836	10,718 ± 247	10,718	<1,000,000	N.D.	11,247 ± 776	37,490
A163T/H256A	TM4/TM6	2.03 ± 0.14	2.4 ± 0.1	2.7	210 ± 19.3	19.6	9.6 ± 2.4	9.6	55.8 ± 15.0	19.2	2.3 ± 0.05	7.7
A163T/N295A	TM4/TM7	1.46 ± 0.28	8.0 ± 2.0	8.9	7788 ± 1332	728	254 ± 8.8	254	740 ± 215	255	212 ± 7.3	707
K199Q/H256A	TM5/TM6	0.91 ± 0.08	23.0 ± 2.1	25.6	102 ± 10.5	9.5	26.8 ± 2.8	26.8	209 ± 14.4	72.1	1.5 ± 0.07	5
H256A/N295A	TM6/TM7	2.98 ± 0.08	21.2 ± 1.7	23.6	191 ± 8.8	17.9	4.3 ± 0.3	4.3	30.4 ± 5.9	10.5	1.3 ± 0.1	4.3

N.D., not determined.

TABLE 2

Ligand-binding properties of the N111G mutant and mutants in the N111G background AT1R

The values are presented as the mean ± S.E.M. of at least three independent experiments performed in duplicate. The effect of the mutations on the binding affinity is expressed as $\Delta K_i = K_i(\text{mutant})/K_i(\text{N111G-AT1})$.

Mutation	Location	B_{max}	Angiotensin II		Losartan		EXP3174		Valsartan		Irbesartan	
			K_i	ΔK_i	K_i	ΔK_i	K_i	ΔK_i	K_i	ΔK_i	K_i	ΔK_i
		pmol/mg	*nM*		*nM*		*nM*		*nM*		*nM*	
N111G	TM3	4.01 ± 0.4	0.01 ± 0.01	1	684 ± 7.9	1	49.9 ± 6.3	1	150 ± 27.4	1	8.2 ± 0.7	1
N111G/V108I	TM3	0.40 ± 0.03	0.02 ± 0.01	1.5	3274 ± 37.7	4.8	212 ± 45.5	4.2	1234 ± 279	8.2	156 ± 21.5	19
N111G/S109T	TM3	0.76 ± 0.31	0.04 ± 0.02	2.6	4338 ± 790	6.3	456 ± 93.2	9.1	5024 ± 347	33.5	365 ± 33.5	44.5
N111G/A163T	TM4	1.56 ± 0.14	0.03 ± 0.02	2.1	1906 ± 43.9	2.8	129 ± 8.9	2.6	419 ± 38.5	2.8	57.9 ± 16.2	7.1
N111G/E173A	ECL2	0.45 ± 0.09	0.02 ± 0.01	1.7	548 ± 177	0.8	30.3 ± 6.9	0.6	157 ± 9.0	1	20.3 ± 2.1	2.5
N111G/F182A	ECL2	1.02 ± 0.13	0.08 ± 0.01	5.5	625 ± 35.9	0.9	47.1 ± 13.2	0.9	196 ± 44.2	1.3	24.5 ± 7.1	3
N111G/Y184A	ECL2	3.23 ± 1.07	0.03 ± 0.02	2.2	503 ± 221	0.7	29.2 ± 10.6	0.6	100 ± 9.2	0.7	4.8 ± 0.7	0.6
N111G/K199A	TM5	0.33 ± 0.03	0.21 ± 0.01	15.3	2069 ± 119	3	282 ± 72.9	5.6	2362 ± 457	15.7	25.2 ± 2.3	3.1
N111G/K199Q	TM5	0.89 ± 0.40	0.01 ± 0.01	0.7	626 ± 245	0.9	145 ± 10.0	2.9	879 ± 121	5.9	6.4 ± 1.1	0.8
N111G/H256A	TM6	0.36 ± 0.04	0.02 ± 0.004	1.1	233 ± 62.6	0.3	10.8 ± 2.4	0.2	87.4 ± 14.9	0.6	2.7 ± 0.1	0.3
N111G/Q257A	TM6	2.01 ± 0.20	0.57 ± 0.16	40.4	146 ± 40.8	0.2	10.8 ± 3.4	0.2	49.1 ± 11.1	0.3	2.7 ± 0.2	0.3
N111G/Q257E	TM6	0.18 ± 0.08	0.11 ± 0.02	7.9	464 ± 37.3	0.7	46.3 ± 1.6	0.9	255 ± 20.5	1.7	49.0 ± 1.1	6
N111G/Y292A	TM7	1.78 ± 0.43	0.05 ± 0.01	3.8	36.8 ± 9.9	0.1	0.78 ± 0.05	0.02	30.6 ± 10.2	0.2	0.4 ± 0.2	0.05
N111G/N295A	TM7	5.59 ± 0.51	0.15 ± 0.04	10.4	4832 ± 663	7.1	220 ± 25.2	4.4	645 ± 95.9	4.3	70.8 ± 1.6	8.6
N111G/S109T/A163T	TM3/TM4	0.78 ± 0.29	0.03 ± 0.02	2.3	6629 ± 1134	9.7	528 ± 60.6	10.6	2737 ± 282	18.2	202 ± 7.0	24.6
N111G/S109T/H256A	TM3/TM6	0.42 ± 0.01	0.04 ± 0.02	2.6	1859 ± 380	2.7	146 ± 44.1	2.9	3209 ± 258	21.4	30.1 ± 3.8	3.7
N111G/S109T/N295A	TM3/TM7	1.86 ± 0.48	0.09 ± 0.03	6.6	37,400 ± 4287	54.7	3942 ± 227	79	58,678 ± 7392	391.2	1976 ± 114	241
N111G/A163T/H256A	TM4/TM6	0.29 ± 0.08	0.07 ± 0.03	4.7	1301 ± 179	1.9	143 ± 35.3	2.9	274 ± 49.9	1.8	26.2 ± 9.2	3.2
N111G/A163T/N295A	TM4/TM7	1.43 ± 0.45	0.31 ± 0.08	21.9	15,043 ± 1553	22	1320 ± 60.7	26.5	3702 ± 466	24.7	156 ± 17.9	19
N111G/K199Q/H256A	TM5/TM6	1.65 ± 0.33	0.16 ± 0.04	11.5	924 ± 53.1	1.4	322 ± 33.2	6.5	4676 ± 695	31.2	34.0 ± 3.1	4.1
N111G/H256A/N295A	TM6/TM7	0.28 ± 0.01	0.31 ± 0.01	22.1	501 ± 74.4	0.7	34.1 ± 6.6	0.7	120 ± 17.9	0.8	1.3 ± 0.2	0.2

are assessed in this study. The Y113A, F182A, Y184A, K199A, K199Q, and N295A mutants reduced binding affinity for Ang II, which was not altered by any of the other mutants.

The V108I, S109T, Y113A, A163T, Q257E, Y292A, and N295A mutants reduced binding affinity for all four ARBs. The K199A and Q257A mutants reduced binding affinity for Losartan, EXP3174, and Valsartan. The K199Q mutant reduced binding affinity for Valsartan. The Y184A mutant increased binding affinity for Irbesartan. All other mutants demonstrated an unaltered binding affinity for all four ARBs. These results indicate that the residues Val108, Ser109, Tyr113, Ala163, Gln257, Tyr292, and Asn295 constitute a common pocket for the binding of all four ARBs. The residue Tyr184 is specific for the binding of Irbesartan and the residue Lys199 is specific for the binding of Losartan, EXP3174, and Valsartan in WT-AT1.

To unravel the putative interactions between the residues involved in the binding of the four ARBs in WT-AT1, the effects of seven double mutants on the binding affinity for the four ARBs were examined (Table 1). Since the ARB binding site residues $Ser109^{TM3}$, $Ala163^{TM4}$, $Lys199^{TM5}$, $His256^{TM6}$, and $Asn295^{TM7}$ in the AT1R are located on different transmembrane (TM) helices, we selected combinations of S109T, A163T, K199Q, H256A, and N295A mutants to evaluate the combined effect of different TM helices for both binding affinity and inverse agonism. The S109T/N295A, A163T/N295A, and K199Q/H256A mutants synergistically reduced binding affinity for all four ARBs. In contrast, the S109T/A163T and S109T/H256A mutants did not show a combined effect on the binding affinity for any of the four ARBs. These results indicate that the combinational interactions between Ser109 and Asn295, between Ala163 and Asn295, and between Lys199 and His256 are possibly important for the binding of all four ARBs in WT-AT1. It is interesting that K199Q and H256A do not change Irbesartan binding individually.

Residues Specific for Binding of Ligands in N111G-AT1. To identify the residues specific for the binding of ligands in N111G-AT1, the effects of various mutants introduced in the N111G-AT1 background (N111G-BG) on the binding affinity of the ligands were examined (Table 2). Since the N111G/Y113A mutant did not show any detectable radioligand-binding activity, the effect of this mutant could not be examined. The N111G/F182A, N111G/K199A, and N111G/N295A mutants reduced binding affinity for Ang II. In addition, N111G/Q257A and N111G/Y292A mutants also reduced binding affinity for Ang II in N111G-BG, which is quite different from those observed in WT-BG. The N111G/Y184A and N111G/K199Q mutants did not alter binding affinity for Ang II.

The effects of most of the mutants on the binding affinity of the ARBs in N111G-BG were quite different from those observed in WT-BG. The N111G/V108I, N111G/S109T, N111G/K199A, and N111G/N295A mutants reduced binding affinity for all four ARBs, while the N111G/E173A and N111G/Y184A mutants did not show an altered binding affinity for all four ARBs. However, the effects of other mutants in the N111G-BG were different from those observed in WT-BG. The N111G/K199Q mutant reduced binding affinity for Valsartan but not for the other ARBs. The binding affinity for Irbesartan was reduced by two additional mutations, N111G/A163T and N111G/F182A. Contrary to that observed for the Q257A and Y292A mutants, the N111G/Q257A and N111G/Y292A mutants increased binding affinity for all four ARBs. These results indicate that the residues Val108, Ser109, Lys199, and Asn295 are common for the binding of all four ARBs, while Ala163 and Phe182 are specific for the binding of Irbesartan in N111G-AT1.

To unravel the putative interactions between the residues involved in the binding of the four ARBs in N111G-AT1, we examined the effects of seven triple mutants on the binding affinity for the four ARBs (Table 2). The N111G/S109T/N295A mutant synergistically reduced binding affinity for all four ARBs. The N111G/S109T/A163T, N111G/S109T/H256A, and N111G/A163T/H256A mutants did not show any combined effects on the binding affinity for all four ARBs. The effects of the other mutants in N111G-BG on the binding affinity for the ARBs were partially different from those observed in WT-BG. The N111G/A163T/N295A mutant synergistically reduced binding affinity for Losartan, EXP3174, and Valsartan, and additively reduced binding affinity for Irbesartan. The N111G/K199Q/H256A mutant synergistically reduced binding affinity for EXP3174, Valsartan, and Irbesartan. These results indicate that the combinational interactions between Ser109 and Asn295 and between Ala163 and Asn295 are important for the binding of all four ARBs, while those between Lys199 and His256 are important for the binding of EXP3174, Valsartan, and Irbesartan in N111G-AT1.

Mutations Affecting the Inverse Agonism of the ARBs in WT-AT1. To identify the residues responsible for the inverse agonism of the ARBs in the WT-AT1, the effects of various mutants introduced in WT-BG on inverse agonism were examined. The V108I, S109T, A163T, E173A, F182A, Q257A, Y292A, and N295A mutants demonstrated sufficient constitutive activity (Supplemental Fig. 2A), and thus the effects of these mutants on the inverse agonism were examined (Fig. 3). Since the Y113A, K199A, K199Q, and H256A mutants displayed only a modest constitutive activity, the effects of these mutants on the inverse agonism could not be examined. The S109T, Y292A, and N295A mutants significantly attenuated inverse agonism for all four ARBs. The V108I mutant significantly attenuated inverse agonism for Losartan and EXP3174. The attenuating effect of V108I on the inverse agonism for Valsartan and Irbesartan was not statistically significant. The E173A mutant significantly attenuated inverse agonism for EXP3174 and attenuated —although not significant statistically—inverse agonism for Losartan. The F182A mutant significantly attenuated inverse agonism for EXP3174, Valsartan, and Irbesartan and attenuated —although not significant statistically—inverse agonism for Losartan. The Q257A mutant significantly attenuated inverse agonism for Losartan, EXP3174, and Valsartan. Other mutants did not alter inverse agonism by any of four ARBs. These results suggest that the residues Val108, Ser109, Phe182, Tyr292, and Asn295 are responsible for the inverse agonism of all four ARBs; the residue Gln257 is responsible for the inverse agonism of Losartan, EXP3174, and Valsartan; and the residue Glu173 is responsible for the inverse agonism of Losartan and EXP3174 in WT-AT1. Note that Phe182 influences inverse agonism without having a significant effect on binding (see *Discussion*).

To determine the combinational interactions between the residues responsible for the inverse agonism in WT-AT1, the effects of three double mutants on the inverse agonism were

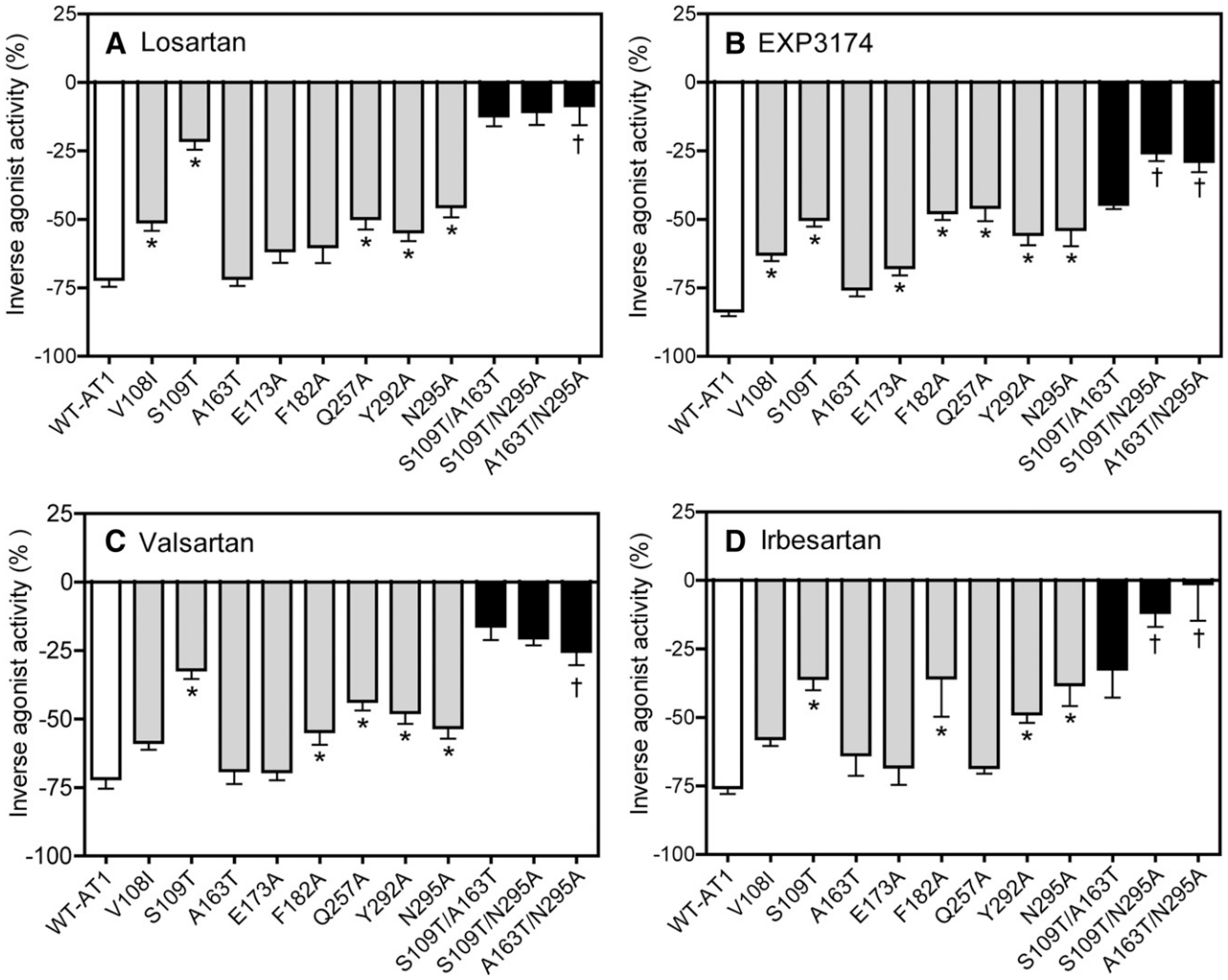

Fig. 3. Effects of the mutants on the inverse agonism of four ARBs in the WT-BG cells as measured by IP assay. The inverse agonist activity of Losartan (A), EXP3174 (B), Valsartan (C), and Irbesartan (D) at a concentration of 10 μM of each ARB in the COS1 cells transfected with WT-AT1 (white bars), single mutants (gray bars), and double mutants (black bars) is shown. Double mutants were constructed using two independent mutants that significantly attenuated the inverse agonist activity. Inverse agonist activity is expressed as the percentage of the constitutive activity of either WT-AT1 or each mutant. The constitutive activity of the vehicle-treated WT-AT1 cells and each mutant is defined as 0%, respectively. *$P < 0.05$ versus WT-AT1; †, additive effect. Gray and black bars indicate single and double mutants, respectively.

examined. The S109T/A163T, S109T/N295A, and A163T/N295A mutants demonstrated sufficient constitutive activity (Supplemental Fig. 3A), and thus the effect of these mutants on the inverse agonism were examined (Fig. 3). The A163T/N295A mutant additively attenuated inverse agonism for all four ARBs. The S109T/N295A mutant additively attenuated inverse agonism for EXP3174 and Irbesartan. The S109T/A163T mutant did not demonstrate any combined effects on the inverse agonism of any of the four ARBs. These results suggest that the combination of Ala163 and Asn295 is important for the inverse agonism of all four ARBs, while those between Ser109 and Asn295 are important for the inverse agonism of EXP3174 and Irbesartan in WT-AT1.

Mutations Affecting the Inverse Agonism of the ARBs in N111G-AT1. The effects of various mutants introduced in N111G-BG on the inverse agonism were examined. All mutants showed significantly higher constitutive activity than WT (Supplemental Fig. 2B), and thus the effects of these mutants on the inverse agonism of the four ARBs were examined (Fig. 4). The effects of different mutants on the inverse agonism of the four ARBs in N111G-BG were quite different from those observed in WT-BG.

The N111G/V108I mutant abolished inverse agonism for Irbesartan and shifted efficacy from inverse agonism toward agonism for Losartan, EXP3174, and Valsartan. The N111G/S109T mutant significantly attenuated inverse agonism for EXP3174, Valsartan, and Irbesartan, but not for Losartan. The N111G/A163T mutant significantly attenuated inverse agonism for EXP3174 and shifted efficacy toward agonism for Losartan and Irbesartan. The N111G/E173A mutant significantly attenuated inverse agonism for EXP3174 and modestly attenuated inverse agonism for Losartan. The N111G/F182A mutant significantly attenuated inverse agonism for EXP3174. However, the N111G/F182A mutant switched the efficacy toward agonism for Losartan and Irbesartan. The N111G/K199A mutant significantly potentiated inverse agonism for all four ARBs and the N111G/K199Q mutant significantly potentiated inverse agonism for Losartan, Valsartan, and Irbesartan. A previous study reported that the N111G/K199Q mutant attenuated inverse agonism for

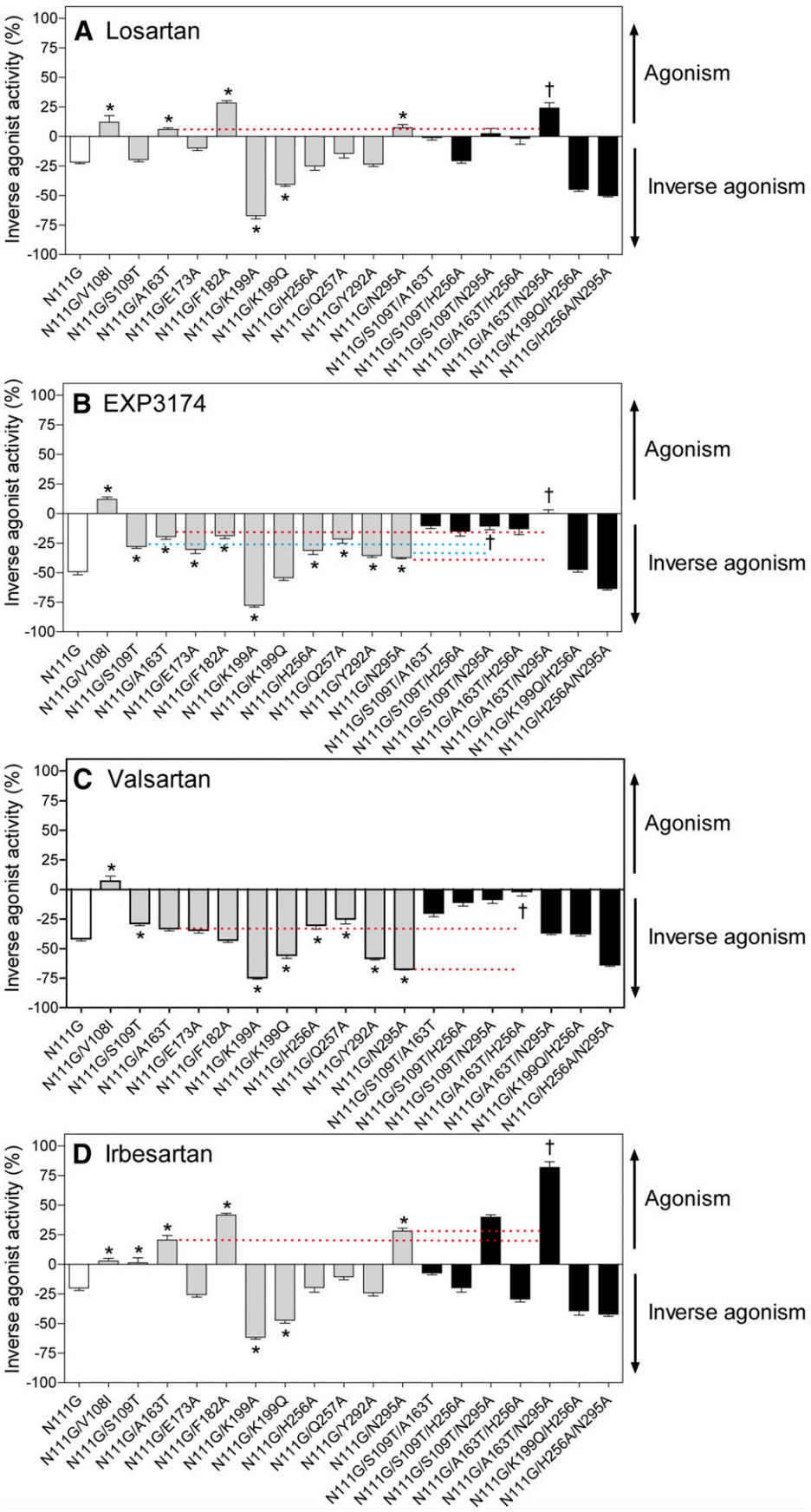

Fig. 4. Effects of the mutants on the efficacy of four ARBs in the N111G-BG cells. The efficacy (inverse agonism or efficacy switch from inverse agonism toward agonism) of Losartan (A), EXP3174 (B), Valsartan (C), and Irbesartan (D) at a concentration of 10 μM of each ARB in COS1 cells transfected with N111G-AT1 (white bars), single mutants in N111G-BG (gray bars), and double mutants in N111G-BG (black bars) is shown. Double mutants in the N111G-BG cells were constructed using the N111G mutant with two additional independent mutants that significantly attenuated the inverse agonist activity or switched efficacy from inverse agonism toward agonism. Agonist activity and inverse agonist activity are expressed as the percentage of the constitutive activity of the vehicle-treated N111G-AT1 cells and each mutant in N111G-BG, respectively. The constitutive activity of the vehicle-treated N111G-AT1 cells and each mutant in N111G-BG is defined as 0%, respectively. *$P < 0.05$ versus N111G-AT1; †, additive effect. Gray and black bars indicate single and double mutants, respectively.

Valsartan (Miura et al., 2008); the reason for the difference is unclear at this time. The N111G/H256A mutant significantly attenuated inverse agonism for EXP3174 and Valsartan. The N111G/Q257A mutant significantly attenuated inverse agonism for EXP3174 and Valsartan, but did not exhibit an altered inverse agonism for Losartan and Irbesartan. The N111G/Y292A mutant significantly attenuated inverse agonism for EXP3174; however, unlike the Y292A mutant, the N111G/Y292A mutant did not exhibit an altered inverse agonism for Losartan and Irbesartan and unexpectedly potentiated the inverse agonism of Valsartan. The N111G/N295A mutant significantly attenuated inverse agonism for EXP3174; however, unlike the N295A mutant, the N111G/N295A mutant shifted efficacy toward agonism for Losartan and Irbesartan and unexpectedly potentiated the inverse agonism of Valsartan.

These results suggest that Val108 influences the inverse agonism of Irbesartan and the efficacy switch from inverse agonism toward agonism for Losartan, EXP3174, and Valsartan. Ser109 affects the inverse agonism of EXP3174, Valsartan and Irbesartan. Ala163, Phe182, and Asn295 affect the inverse agonism of EXP3174 and modulate the efficacy switch from inverse agonism toward agonism for Losartan and Irbesartan. Glu173 influences the inverse agonism of Losartan and EXP3174. Gln257 influences the inverse agonism of EXP3174 and Valsartan. Finally, Tyr292 affects the inverse agonism of EXP3174 in N111G-AT1.

To determine the combinational interactions between the residues responsible for the inverse agonism in N111G-AT1, the effects of seven triple mutants on the inverse agonism were examined. The N111G/S109T/A163T, N111G/S109T/H256A, N111G/S109T/N295A, N111G/A163T/H256A, N111G/A163T/N295A, N111G/K199Q/H256A, and N111G/H256A/N295A mutants demonstrated sufficient constitutive activity (Supplemental Fig. 3A), and thus the effect of these mutants on the inverse agonism were examined (Fig. 4). The N111G/S109T/N295A mutant, as well as the S109T/N295A mutant, additively attenuated inverse agonism for EXP3174. The N111G/A163T/H256A mutant additively attenuated inverse agonism for Valsartan. The N111G/A163T/N295A mutant, as well as the A163T/N295A mutant, additively attenuated inverse agonism for EXP3174; however, unlike the A163T/N295A mutant, the N111G/A163T/N295A mutant additively potentiated the efficacy switch from inverse agonism toward agonism for Losartan and Irbesartan. No other triple mutants exhibited combined effects on the inverse agonism of any of the four ARBs. These results suggest that the combinational interactions between Ser109 and Asn295 are important for the inverse agonism of EXP3174, while those between Ala163 and His256 are important for the inverse agonism of Valsartan and those between Ala163 and Asn295 are important for the inverse agonism of EXP3174 and the efficacy switch from inverse agonism toward agonism for Losartan and Irbesartan in N111G-AT1.

Molecular Model of ARB/WT-AT1 Complexes. To examine whether the residues targeted in our study do actually interact with the four ARBs, molecular models of the AT1R were employed. The molecular models we used were developed based on the crystal structure data of human AT1R bound to an experimental hypertensive agent ZD7155 [5,7-diethyl-3,4-dihydro-1-[[2′-(1*H*-tetrazol-5-yl)[1,1′-biphenyl]-4-yl]methyl]-1,6-naphthyridin-2(1*H*)-one hydrochloride] (see Fig. 5A), as described in *Materials and Methods* (Zhang et al., 2015). We used the human AT1R structure since the overall sequence homology of rat and human AT1Rs is 95% and all the residues examined in this study are the same as in the residues of the human AT1R. Moreover, the sequence of the crystalized human AT1R portion and rat AT1R are identical. Therefore, it was more reliable to model the human AT1R for the sake of linking our study to human health relevance, especially when ARB docking is addressed. Figure 5A depicts the ARB binding site observed in the crystal structure of the AT1R, which consists of all seven TM helices and extracellular loops 1 and 2. The four individual ARB/AT1R complexes are shown in Fig. 5, B–E. The binding poses for the four ARBs in the AT1R were predicted by energy-based docking simulation studies. The nature of the interactions with the AT1R is different for each ARB due to their distinct chemical structures. However, all four compounds bind in similar orientations and engage in interactions with the critical residue $Arg167^{ECL2}$. In previous mutagenesis studies, we mutated the Arg167 to Ala, Gln, and His and examined the binding affinity of Ang II and several ARBs for these mutants. These mutants markedly reduced the binding affinity for all ligands (Noda et al., 1995; Takezako et al., 2004; Zhang et al., 2015). These studies have already validated the critical requirement of $Arg167^{ECL2}$ for binding all ARBs and Ang II. Therefore, we did not mutate Arg167 in the present study in order to avoid duplication of negative binding results. Out of the 12 residues examined in this study, Val108, Ser109, Tyr113, Ala163, Phe182, Tyr184, Lys199, His256, Gln257, Tyr292, and Asn295 were present in the common ARB-binding pocket. One residue, Glu173, lacks reliable X-ray diffraction density in the AT1R structure; therefore, we did not indicate this residue in Fig. 5, B–E.

The canonical ARB binding pocket of the AT1R (Fig. 5; Zhang et al., 2015) consists of interacting residues of TM helices I-VII as well as mainly from the second extracellular loop (ECL2). The tetrazole group, a common acidic moiety present in all four ARBs, bonds with Arg167 in ECL2, which is not targeted in this study, hence not shown in Fig. 5. The canonical ARB binding pocket includes contacts mediated by residues, including $Val108^{TM3}$, $Ser109^{TM3}$, $Ala163^{TM4}$, $Gln257^{TM6}$, $Tyr292^{TM7}$, and $Asn295^{TM7}$. The ARB docking results suggest that the flexible side chain of $Lys199^{TM5}$ retains some conformational heterogeneity in the AT1R that the amino group of this residue can form salt bridges with acidic moieties of ARBs or participate in water-mediated interactions with the biphenyl scaffold in ARBs. This entropic state of $Lys199^{TM5}$ partly explains the variable role this residue seems to play in previous studies (Takezako et al., 2004; Miura et al., 2006, 2008, 2013). The residues $Tyr113^{TM3}$, $Phe182^{ECL2}$, $Tyr184^{ECL2}$, and $His256^{TM6}$ may hydrophobically interact with ARBs in the AT1R ligand-binding pocket. The complex structures show that the imidazole ring of Losartan and EXP3174 and equivalent substituents in Valsartan and Irbesartan interact with the floor of the ligand pocket, including residues $Tyr292^{TM7}$ and $Asn295^{TM7}$. The biphenyl rings of ARBs interact with $Val108^{TM3}$ and $Ser109^{TM3}$ as well as with $Trp253^{TM6}$ and $Gln257^{TM6}$. Thus, the residues targeted in this study along with $Arg167^{ECL2}$ define the unique shape of the AT1R ligand-binding pocket. The distances and angles of the different bonding interactions

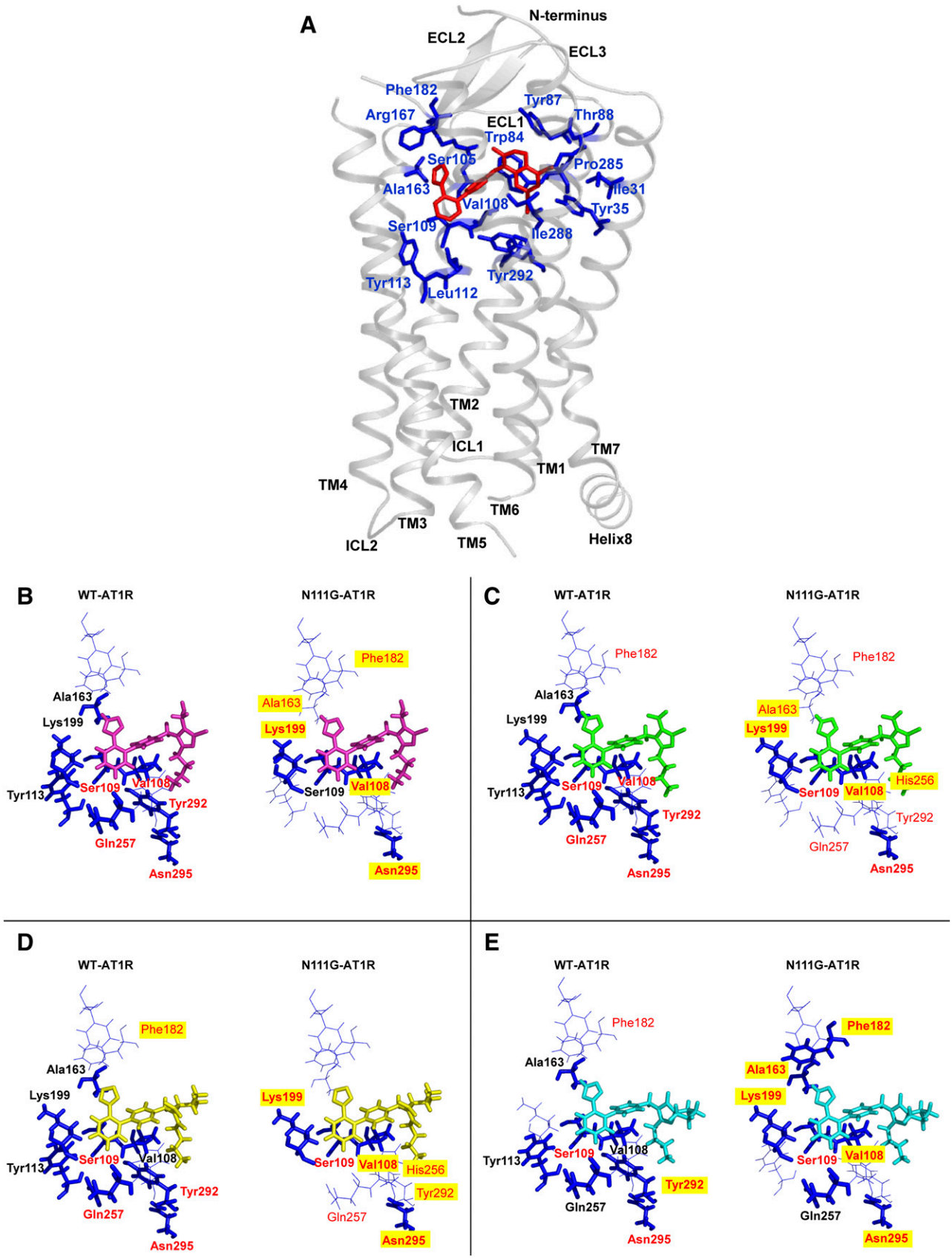

Fig. 5. Human AT1R structure showing details of the ligand, ZD7155 interactions with specific residues (A). Models of the AT1R binding pocket interaction with Losartan (B), EXP3174 (C), Valsartan (D), and Irbesartan (E). Side-chain positions for the residues studied are located within a 10 Å pocket for each ARB. In each ARB-bound model, the side-chain single mutations affecting binding with >3-fold change of K_i are indicated by the blue color and bold labels, both in the ground state (WT-AT1) and activated state (N111G-AT1). A residue label in red indicates a significant effect on the

differ, which may explain the differences in the binding affinity and pharmacological properties of the four ARBs at the AT1R. For instance, the docking results suggest that Losartan, the clinically used ARB for treatment of hypertension with a weak inverse agonist and lower binding affinity to AT1R forms only a salt bridge with Arg167^{ECL2} through the tetrazole moiety and lacks polar interactions with other residues. The active metabolite of Losartan, EXP3174, a better binder and stronger inverse agonist (Takezako et al., 2004), binds in a similar way as Losartan; however, its carboxyl group could engage in an additional salt bridge interaction with Arg167^{ECL2}.

Superposition of Binding and Inverse Agonism Data in the ARB/N111G-AT1 Complex. Modeling the active state of N111G-AT1R was problematic, as has been reported for many other GPCRs, because the long timescale required for molecular dynamics simulations is untenable (Manglik and Kobilka, 2014). Short-time simulation efforts showed modest changes in the biding pocket in the AT1R with low *P* values. In addition, comparison of multiple active and inactive crystal structures of GPCRs have been reported to show only modest changes in the binding pocket residues in each receptor, and the two states are remarkably similar in the ligand-binding pocket (Katritch et al., 2013). Therefore, we color-highlighted residues based on the experimental data for each ARB in the ground and active states as indicated in Fig. 5, B–E.

Superposition of the experimental data for WT-AT1 and N111G-AT1 binding and inverse agonism is shown in Fig. 5. Different residues affect both measured properties of ARBs, suggesting subtle movement of the TM helices and extracellular loop regions in N111G-AT1 for all four ARBs. In the WT background, residues Ser109^{TM3}, Tyr292^{TM7}, and Asn295^{TM7} are essential for inverse agonism of all four ARBs, and Gln257^{TM6} and Phe182^{ECL2} are essential for three out of four ARBs. In contrast, in the N111G-AT1 a completely different set of interactions mediates inverse agonism. While Val108^{TM3} and Lys199^{TM5} are essential for the inverse agonism of all four ARBs, Ser109^{TM3}, Ala163^{TM4}, Phe182^{ECL2}, Tyr292^{TM7}, and Asn295^{TM7} affect inverse agonism of three out of four ARBs.

Discussion

Our data confirm the inverse agonist property of the four biphenyl-tetrazole ARBs, Losartan, EXP3174, Valsartan, and Irbesartan, for both ground (WT) and constitutively activated (N111G-AT1) states of AT1R. Our data validate previous observations that the inverse agonism potency of ARBs is attenuated during the transition of the AT1R toward the activated state (Noda et al., 1996; Le et al., 2003; Miura et al., 2006, 2008). We herein propose a potential molecular mechanism for this phenomenon.

Mechanism of the Inverse Agonism of ARBs for AT1R in the Ground State. The molecular models suggest that all of the residues examined potentially interact with the ARBs. The contribution of different residues to binding and inverse agonism could differ due to the distances and angles of different bonding interactions, which differ based on the unique chemical structure of each ARB. The differences in binding affinity and inverse agonism potential of ARBs at the AT1R must be based on the differences in energy gained through their bonding with residues. In view of this, our experiments identified Ser109^{TM3}, Tyr292^{TM7}, and Asn295^{TM7} as common residues essential for the inverse agonism of all four ARBs and Gln257^{TM6} and Phe182^{ECL2} are essential for three out of four ARBs. Out of these, four residues also significantly affect binding affinity, thus confirming a direct relationship between binding and inverse agonism in the ground state. Phe182^{ECL2} seems to be an exception; this residue does not significantly affect K_i but affects inverse agonism, which may be due to its location in a dynamic portion of the AT1R, as suggested previously (Unal et al., 2010, 2013) and confirmed by the X-ray structure of the AT1R (Zhang et al., 2015). The influence of residues located in the dynamic region of the receptor may be reflected in the prolonged functional assay at 37°C rather than in the shorter time binding assay at room temperature.

Since mutations of either Asn111^{TM3} or Asn295^{TM7} induce constitutive activation of the AT1R, the inactive conformation of AT1R was proposed to be stabilized by the H-bond between Asn111^{TM3} and Asn295^{TM7}, which is confirmed by the crystal structure (Zhang et al., 2015). Ligand activation of the WT receptor disrupts this H-bond, leading Asn295^{TM7} to interact with the conserved Asp74^{TM2}. The Asp74^{TM2}-Asn111^{TM3}-Asn295^{TM7} H-bond network in the active state involves additional residues, Trp253^{TM6} from the toggle-switch motif (Ahuja and Smith, 2009; Holst et al., 2010); Phe77^{TM2}, Val108^{TM3}, Ile288^{TM7} and Tyr292^{TM7}; and Asn298^{TM7} from the NPxxY motif (Cabana et al., 2013; Zhang et al., 2015). Thus, the network of interacting residues around Asn111^{TM3} and Asn295^{TM7} play an essential role in AT1R activation, probably by relaying the conformational changes in the ligand-binding pocket to the cytoplasmic domain coupling to the G proteins. This network may also impact the interhelical interactions required for the binding and functional properties of ARBs as well the consequent inactivation of the AT1R. We propose that the observed direct interaction of the ARBs with the residues Ser109^{TM3}, Gln257^{TM6}, Tyr292^{TM7}, and Asn295^{TM7} constrains this network, thereby leading to stabilizing the inactive state of the receptor, i.e., inverse agonism. All residues involved in the inverse agonism of the ARB in the AT1R are conserved at the equivalent position in many GPCRs, implying that this may be a general mechanism for inverse agonists. However, the role played by Phe182^{ECL2} in the inverse agonism of ARBs may be unique to the AT1R, which seems to be supported by previous functional studies (Unal et al., 2010, 2013) and by the X-ray structure of the AT1R (Zhang et al., 2015).

Mechanism of the Attenuated Inverse Agonism of ARBs for the Activated State AT1R. In the activated mutant N111G-AT1, the H-bond network and residues contributing to inverse agonism are different. Mutations of Val108^{TM3} and Lys199^{TM5} affect the inverse agonism of all four ARBs, while five different residues, Ser109^{TM3}, Ala163^{TM4}, Phe182^{ECL2}, Tyr292^{TM7}, and Asn295^{TM7}, affect the inverse agonism of three out of four ARBs. Losartan

inverse agonism for IP formation in the ground state (WT-AT1) and activated state (N111G-AT1). Highlighted residues depict unique influence on inverse agonism for IP formation in the specified state of the AT1R for the particular ARB.

inverse agonism involves interaction with TM3, TM4, ECL2, TM5, and TM7 in the activated state, while in the ground state it involves interaction with TM helices 3, 6, and 7. The EXP3174 inverse agonism involves interaction with TM3, TM4, ECL2, TM5, TM6, and TM7 in N111G-AT1, while in the ground state it involves interaction with TM helices 3, 6, 7, and ECL2. Inverse agonism of Valsartan involves interaction with TM helices 3, 5, 6, and 7 in N111G-AT1, while in the ground state it involves interaction with TM3, ECL2, TM6, and TM7. Irbesartan inverse agonism involves interaction with TM3, TM4, ECL2, TM5, and TM7 in N111G-AT1, while in the WT it involves interaction with TM3, ECL2, and TM7. These comparisons suggest that leaning of ARBs on TM helices and ECL2 changes in the activated state from the ground state of the AT1R. More residues appear to be involved in the inverse agonist response, independent of the binding affinity in the activated state (see Fig. 5), suggesting a more dynamic interaction of these residues akin to that observed for Phe182^{ECL2} in the ground state, which is thought to be due to conformational flexibility. Much evidence for conformational changes in the ligand-binding pocket in the activated state compared with the inactive state has been identified in the case of the agonist-bound β2 adrenergic receptor, light-activated rhodopsin, the constitutively active rhodopsin mutant, and the agonist-bound adenosine A2A receptor (Choe et al., 2011; Lebon et al., 2011; Rasmussen et al., 2011; Standfuss et al., 2011). By analogy to these GPCRs, we suggest that the active state of the AT1R harbors conformational changes in the ligand-binding pocket. Furthermore, direct structure-function studies on the AT1R have suggested both rotational and translational motion of TM2, TM3, TM5, TM6, and TM7 in the N111G-AT1R (Boucard et al., 2003; Martin et al., 2004, 2007; Domazet et al., 2009). Based on molecular dynamics simulation studies on N111G-AT1R, an active-state H-bond network where Asp74^{TM2} interacts with Asn46^{TM1} and Asn295^{TM7} was proposed (Cabana et al., 2013). The same authors also indicated that the N111G mutation leads to hydrating the hydrophobic core and facilitating the interaction of the toggle switch residue, Trp253^{TM6} with Ala291^{TM7} and Leu112^{TM3} (Cabana et al., 2013). All four ARBs may thus prevent stability of the Asn46-Asp74-Asn295 H-bond network and reduce hydration of the transmembrane core through their hydrophobic characteristics.

Essential Role of the ECL2 in the Regulation of the AT1R Conformational States. The crystal structure indicates that residues Glu173^{ECL2} and Phe182^{ECL2} are within 10 Å of the binding location of all four ARBs, clearly providing structural basis for the E173A and N111G/E173A mutants in the attenuated inverse agonism of Losartran and EXP3174, and the F182A mutant attenuated inverse agonism of all four ARBs. Furthermore, the most critical interaction of tetrazole with Arg168 in this loop suggests that ARBs modulate ECL2 conformation directly in the AT1R (Zhang et al., 2015). ECL2 is known as an important regulator for ligand entry and the receptor function in various GPCRs (Shi and Javitch, 2004; Scarselli et al., 2007). In the AT1R, the ECL2 was shown to assume an open conformation in the ligand free state, and to assume a lid conformation in the Losartan-bound state, Candesartan-bound state, and Ang II–bound state (Unal et al., 2010, 2013). These studies suggest that the ECL2 regulates the conformational state of the AT1R. The data in the present study indicate that the ECL2 residues Glu173 and Phe182 are important regulators of conformation for inverse agonism of ARBs for the AT1R.

Residues Switching Efficacy toward Agonism in the Activated State of AT1R. We observed that substitution of Val108^{TM3}, Ala163^{TM4}, Asn295^{TM7}, and Phe182^{ECL2} switched efficacy toward agonism for the ARBs in the activated state but not in the ground state (Fig. 4). Although the exact mechanism for the change of the ligand-based function of the receptor is unclear, a possible mechanism for this phenomenon is described subsequently. Bulky substitution of Val108 and Ala163 may cause steric hindrance in the ARB-induced inactive-state transition (which may hydrate the hydrophobic core) and in the stabilization of the Asn46-Asp74-Asn295 H-bond network. On the other hand, Ala substitution for Asn295 and Phe182 may weaken the interaction with the ARBs (which may also hydrate the hydrophobic core) and the stabilization of the Asn46-Asp74-Asn295 H-bond network. However, elucidating the precise mechanism of such a transformation of pharmacological behavior of ligands needs additional biophysical experiments, such as visualization of bound water molecules in active and inactive states. The current resolution of the AT1R structure is not sufficient for this type of analysis. Saturation mutagenesis at Val108, Ala163, Asn295, and Phe182 sites combined with binding affinity and receptor activity assessment may be an alternate, but indirect, method that would elucidate the potential mechanism for this phenomenon. Ultimately, both types of analyses are essential to provide insights into the regulatory mechanism of the GPCR function.

Conclusions. Our findings provide significant information that could be useful in developing novel ARBs as well as improving the inverse agonism efficacy of currently used ARBs for the active state of the AT1R. Novel ARBs could be more therapeutically relevant than the current commercially available ARBs in treating clinical conditions in which ligand-independent activation of the AT1R may be prevalent, such as hypertension, preeclampsia, and renal transplantation. Finally, our findings provide new insight into the essential role of the ECL2 residues Glu173 and Phe182 for the regulation of the conformational states of the AT1R and the potential for developing a new class of ARBs that directly targets the ECL2. Further studies are needed to identify the precise role of the residues in the ECL2 for the regulation of the conformational states of the AT1R.

Authorship Contributions

Participated in research design: Takezako, Karnik.

Conducted experiments: Takezako.

Contributed new reagents or analytic tools: Takezako, Unal, Karnik.

Performed data analysis: Takezako, Unal, Karnik.

Wrote or contributed to the writing of the manuscript: Takezako, Unal, Karnik, Node.

References

Abagyan RA and Totrov MM (1997) Contact area difference (CAD): a robust measure to evaluate accuracy of protein models. *J Mol Biol* **268:**678–685.

Ahuja S and Smith SO (2009) Multiple switches in G protein-coupled receptor activation. *Trends Pharmacol Sci* **30:**494–502.

Baleanu-Gogonea C and Karnik S (2006) Model of the whole rat AT_1 receptor and the ligand-binding site. *J Mol Model* **12:**325–337.

Boucard AA, Roy M, Beaulieu ME, Lavigne P, Escher E, Guillemette G, and Leduc R (2003) Constitutive activation of the angiotensin II type 1 receptor alters the spatial proximity of transmembrane 7 to the ligand-binding pocket. *J Biol Chem* **278:**36628–36636.

Cabana J, Holleran B, Beaulieu ME, Leduc R, Escher E, Guillemette G, and Lavigne P (2013) Critical hydrogen bond formation for activation of the angiotensin II type 1 receptor. *J Biol Chem* **288:**2593–2604.

Choe HW, Kim YJ, Park JH, Morizumi T, Pai EF, Krauss N, Hofmann KP, Scheerer P, and Ernst OP (2011) Crystal structure of metarhodopsin II. *Nature* **471:** 651–655.

Domazet I, Martin SS, Holleran BJ, Morin ME, Lacasse P, Lavigne P, Escher E, Leduc R, and Guillemette G (2009) The fifth transmembrane domain of angiotensin II Type 1 receptor participates in the formation of the ligand-binding pocket and undergoes a counterclockwise rotation upon receptor activation. *J Biol Chem* **284:**31953–31961.

Fredriksson R, Lagerström MC, Lundin LG, and Schiöth HB (2003) The G-protein-coupled receptors in the human genome form five main families. Phylogenetic analysis, paralogon groups, and fingerprints. *Mol Pharmacol* **63:**1256–1272.

Garland SL (2013) Are GPCRs still a source of new targets? *J Biomol Screen* **18:** 947–966.

Gosselin MJ, Leclerc PC, Auger-Messier M, Guillemette G, Escher E, and Leduc R (2000) Molecular cloning of a ferret angiotensin II AT_1 receptor reveals the importance of position 163 for Losartan binding. *Biochim Biophys Acta* **1497:**94–102.

Halgren TA (1995) Potential energy functions. *Curr Opin Struct Biol* **5:**205–210.

Holst B, Nygaard R, Valentin-Hansen L, Bach A, Engelstoft MS, Petersen PS, Frimurer TM, and Schwartz TW (2010) A conserved aromatic lock for the tryptophan rotameric switch in TM-VI of seven-transmembrane receptors. *J Biol Chem* **285:**3973–3985.

Ji H, Leung M, Zhang Y, Catt KJ, and Sandberg K (1994) Differential structural requirements for specific binding of nonpeptide and peptide antagonists to the AT1 angiotensin receptor. Identification of amino acid residues that determine binding of the antihypertensive drug losartan. *J Biol Chem* **269:**16533–16536.

Ji H, Zheng W, Zhang Y, Catt KJ, and Sandberg K (1995) Genetic transfer of a nonpeptide antagonist binding site to a previously unresponsive angiotensin receptor. *Proc Natl Acad Sci USA* **92:**9240–9244.

Katritch V, Cherezov V, and Stevens RC (2013) Structure-function of the G protein-coupled receptor superfamily. *Annu Rev Pharmacol Toxicol* **53:**531–556.

Khan BV (2011) The effect of amlodipine besylate, losartan potassium, olmesartan medoxomil, and other antihypertensives on central aortic blood pressure and biomarkers of vascular function. *Ther Adv Cardiovasc Dis* **5:**241–273.

Le MT, Vanderheyden PM, Szaszák M, Hunyady L, Kersemans V, and Vauquelin G (2003) Peptide and nonpeptide antagonist interaction with constitutively active human AT_1 receptors. *Biochem Pharmacol* **65:**1329–1338.

Lebon G, Warne T, Edwards PC, Bennett K, Langmead CJ, Leslie AGW, and Tate CG (2011) Agonist-bound adenosine A_{2A} receptor structures reveal common features of GPCR activation. *Nature* **474:**521–525.

Lee M, Saver JL, Hong KS, Hao Q, Chow J, and Ovbiagele B (2012) Renin-angiotensin system modulators modestly reduce vascular risk in persons with prior stroke. *Stroke* **43:**113–119.

Manglik A and Kobilka B (2014) The role of protein dynamics in GPCR function: insights from the β2AR and rhodopsin. *Curr Opin Cell Biol* **27:**136–143.

Martin SS, Boucard AA, Clément M, Escher E, Leduc R, and Guillemette G (2004) Analysis of the third transmembrane domain of the human type 1 angiotensin II receptor by cysteine scanning mutagenesis. *J Biol Chem* **279:**51415–51423.

Martin SS, Holleran BJ, Escher E, Guillemette G, and Leduc R (2007) Activation of the angiotensin II type 1 receptor leads to movement of the sixth transmembrane domain: analysis by the substituted cysteine accessibility method. *Mol Pharmacol* **72:**182–190.

Mederos y Schnitzler M, Storch U, and Gudermann T (2011) AT_1 receptors as mechanosensors. *Curr Opin Pharmacol* **11:**112–116.

Miura S, Fujino M, Hanzawa H, Kiya Y, Imaizumi S, Matsuo Y, Tomita S, Uehara Y, Karnik SS, and Yanagisawa H et al. (2006) Molecular mechanism underlying inverse agonist of angiotensin II type 1 receptor. *J Biol Chem* **281:**19288–19295.

Miura S, Kiya Y, Kanazawa T, Imaizumi S, Fujino M, Matsuo Y, Karnik SS, and Saku K (2008) Differential bonding interactions of inverse agonists of angiotensin II type 1 receptor in stabilizing the inactive state. *Mol Endocrinol* **22:** 139–146.

Miura S, Nakao N, Hanzawa H, Matsuo Y, Saku K, and Karnik SS (2013) Reassessment of the unique mode of binding between angiotensin II type 1 receptor and their blockers. *PLoS One* **8:**e79914.

Noda K, Feng YH, Liu XP, Saad Y, Husain A, and Karnik SS (1996) The active state of the AT_1 angiotensin receptor is generated by angiotensin II induction. *Biochemistry* **35:**16435–16442.

Noda K, Saad Y, Kinoshita A, Boyle TP, Graham RM, Husain A, and Karnik SS (1995) Tetrazole and carboxylate groups of angiotensin receptor antagonists bind to the same subsite by different mechanisms. *J Biol Chem* **270:**2284–2289.

Rasmussen SGF, Choi HJ, Fung JJ, Pardon E, Casarosa P, Chae PS, Devree BT, Rosenbaum DM, Thian FS, and Kobilka TS et al. (2011) Structure of a nanobody-stabilized active state of the β_2 adrenoceptor. *Nature* **469:**175–180.

Scarselli M, Li B, Kim SK, and Wess J (2007) Multiple residues in the second extracellular loop are critical for M_3 muscarinic acetylcholine receptor activation. *J Biol Chem* **282:**7385–7396.

Schambye HT, Hjorth SA, Bergsma DJ, Sathe G, and Schwartz TW (1994) Differentiation between binding sites for angiotensin II and nonpeptide antagonists on the angiotensin II type 1 receptors. *Proc Natl Acad Sci USA* **91:**7046–7050.

Shi L and Javitch JA (2004) The second extracellular loop of the dopamine D_2 receptor lines the binding-site crevice. *Proc Natl Acad Sci USA* **101:**440–445.

Standfuss J, Edwards PC, D'Antona A, Fransen M, Xie G, Oprian DD, and Schertler GF (2011) The structural basis of agonist-induced activation in constitutively active rhodopsin. *Nature* **471:**656–660.

Storch U, Mederos y Schnitzler M, and Gudermann T (2012) G protein-mediated stretch reception. *Am J Physiol Heart Circ Physiol* **302:**H1241–H1249.

Takezako T, Gogonea C, Saad Y, Noda K, and Karnik SS (2004) "Network leaning" as a mechanism of insurmountable antagonism of the angiotensin II type 1 receptor by non-peptide antagonists. *J Biol Chem* **279:**15248–15257.

Tuccinardi T, Calderone V, Rapposelli S, and Martinelli A (2006) Proposal of a new binding orientation for non-peptide AT1 antagonists: homology modeling, docking and three-dimensional quantitative structure-activity relationship analysis. *J Med Chem* **49:**4305–4316.

Unal H, Jagannathan R, Bhat MB, and Karnik SS (2010) Ligand-specific conformation of extracellular loop-2 in the angiotensin II type 1 receptor. *J Biol Chem* **285:**16341–16350.

Unal H, Jagannathan R, Bhatnagar A, Tirupula K, Desnoyer R, and Karnik SS (2013) Long range effect of mutations on specific conformational changes in the extracellular loop 2 of angiotensin II type 1 receptor. *J Biol Chem* **288:**540–551.

Unal H, Jagannathan R, and Karnik SS (2012) Mechanism of GPCR-directed autoantibodies in diseases. *Adv Exp Med Biol* **749:**187–199.

Unal H and Karnik SS (2014) Constitutive activity in the angiotensin II type 1 receptor: discovery and applications. *Adv Pharmacol* **70:**155–174.

Vejakama P, Thakkinstian A, Lertrattananon D, Ingsathit A, Ngarmukos C, and Attia J (2012) Reno-protective effects of renin-angiotensin system blockade in type 2 diabetic patients: a systematic review and network meta-analysis. *Diabetologia* **55:**566–578.

Vijayaraghavan K and Deedwania P (2011) Renin-angiotensin-aldosterone blockade for cardiovascular disease prevention. *Cardiol Clin* **29:**137–156.

Wallukat G and Schimke I (2014) Agonistic autoantibodies directed against G-protein-coupled receptors and their relationship to cardiovascular diseases. *Semin Immunopathol* **36:**351–363.

Wei F, Jia XJ, Yu SQ, Gu Y, Wang L, Guo XM, Wang M, Zhu F, Cheng X, and Wei YM et al.; SOT-AT1 Study Group (2011) Candesartan versus imidapril in hypertension: a randomised study to assess effects of anti-AT1 receptor autoantibodies. *Heart* **97:**479–484.

Yamano Y, Ohyama K, Chaki S, Guo DF, and Inagami T (1992) Identification of amino acid residues of rat angiotensin II receptor for ligand binding by site directed mutagenesis. *Biochem Biophys Res Commun* **187:**1426–1431.

Zhang H, Unal H, Gati C, Han GW, Liu W, Zatsepin NA, James D, Wang D, Nelson G, and Weierstall U et al. (2015) Structure of the angiotensin receptor revealed by serial femtosecond crystallography. *Cell* **161:**833–844.

Zou Y, Akazawa H, Qin Y, Sano M, Takano H, Minamino T, Makita N, Iwanaga K, Zhu W, and Kudoh S et al. (2004) Mechanical stress activates angiotensin II type 1 receptor without the involvement of angiotensin II. *Nat Cell Biol* **6:**499–506.

Address correspondence to: Takanobu Takezako, Department of Biosignal Pathophysiology, Kobe University Graduate School of Medicine, 1-1 Rokkodai-cho, Nada-ku, Kobe 657-8501, Japan. E-mail: takezakot@people.kobe-u.ac.jp